

Reliability assessment of shallow foundations on undrained soils considering soil spatial variability

J.T. Simões^a, Luis C. Neves^b, Armando N. Antão^{a,*}, Nuno M. C. Guerra^a

^aUNIC, Department of Civil Engineering, Faculdade de Ciências e Tecnologia, Universidade Nova de Lisboa, Portugal

^bResilience Engineering Research Group, Faculty of Engineering, University of Nottingham, UK

Abstract

Structural design using partial safety factors aims at achieving a homogeneous safety level in geotechnical design without the use of more complex reliability analysis. In this work, the different Design Approaches proposed by Eurocode 7 for shallow foundations resting on the surface of undrained soils are compared in terms of the resulting reliability indices. The influence of both centered and eccentric loads, as well as homogeneous and heterogeneous isotropic and anisotropic distributions for the variability of soil properties were investigated in the reliability analysis.

A finite element implementation of the upper bound theorem of limit analysis is combined with Latin Hypercube sampling to compute the probabilistic response of shallow foundations. Considering realistic probabilistic distributions for both permanent and live loads, First Order Reliability Method is used to calculate the reliability index of such structures designed according to the different Design Approaches present in Eurocode 7.

The results obtained show that the Eurocode 7 leads to satisfactory reliability indices, but that significant differences between Design Approaches exist.

Keywords: Reliability assessment, Eurocode 7, anisotropic soil spatial variability, upper bound theorem, bearing capacity, uncertainty of load eccentricity

1. Introduction

The partial safety factors method is a semi-probabilistic safety verification method aiming at attaining uniform and consistent safety levels, without the complexity of explicit reliability analysis. That approach is employed in Eurocode 7 [11] for geotechnical limit states through the use of three different Design Approaches. These approaches should result in uniform safety levels, consistent with the target reliability indices prescribed in Eurocode 0 [10]. However, the different Design Approaches proposed in Eurocode 7 [11] can, potentially, result in structures with very different levels of safety, and

*Corresponding author

Email addresses: jtbsimoes@gmail.com (J.T. Simões), luis.neves@nottingham.ac.uk (Luis C. Neves), anna@fct.unl.pt (Armando N. Antão), nguerra@fct.unl.pt (Nuno M. C. Guerra)

9 a reliability analysis can assess the consistency of the methods proposed in codes [32,
10 e.g.].

11 In the partial safety factors method, the large uncertainties present in geotechnical
12 design [38, 39, 53, e.g.] are considered through the use of nominal values of properties
13 and safety factors applied to loads, soil properties and resistances [11].

14 The present paper aims at evaluating the reliability of the bearing capacity of shallow
15 foundations under undrained conditions. For such analysis, it is paramount to consider
16 explicitly the uncertainty and heterogeneity characteristics of soils. According to Phoon
17 and Kulhawy [38], uncertainties in soil properties result from (i) inherent variability, (ii)
18 errors in the performed measurements and (iii) errors from transformation of experimen-
19 tal tests results to mechanical properties. It has been shown that uncertainties like the
20 inherent variability can significantly influence the failure mode and the bearing capacity
21 of shallow foundations [22, 23, 19, see e.g.]. Moreover, the uncertainty in loading must
22 also be considered, in particular in what regards the eccentricity of applied loads. In
23 fact, due to uncertainty in the amplitude of different loads, random deviations in the
24 point of application of the resulting load may arise, influencing the failure mode of the
25 foundation and its safety.

26 The collapse load of foundations under these conditions can be computed using dif-
27 ferent numerical approaches. In this paper, bearing capacity is determined using a finite
28 element implementation of the limit analysis upper bound theorem, the Sublim3D code,
29 described in [45]. The ability of the mentioned implementation to compute upper bound
30 solutions of various problems has been previously demonstrated [44, 43, 4]. This code
31 uses a parallel algorithm which significantly reduces the computational time. Calcula-
32 tions were performed in a cluster with 104 cores.

33 The use of advanced numerical methods for computing the collapse load of foundations
34 limits the use of gradient-based reliability methods (*e.g.*, FORM – First Order Reliability
35 Method – and SORM – Second Order Reliability Method), making simulation the most
36 effective tool for reliability assessment. To assess the methodology proposed in Eurocode
37 7 [11], the reliability index of a set of shallow foundations designed according to its three
38 Design Approaches (*DA*) is evaluated. The foundations under analysis are continuous
39 footings on soil responding in undrained conditions. For these, two-dimensional models
40 are usually employed and, due to their lower computational cost, will also be used here.
41 The spatial variability of the soil properties, and therefore its heterogeneity, can be
42 considered using random fields [38, e.g.]. Random fields can be generated using a wide
43 range of approaches [15, 20, 16]. To reduce the number of samples required for achieving
44 acceptable results, Latin Hypercube sampling was employed in this work [34, 21, 36]. This
45 method was also used by Cho and Park [13] to study the same geotechnical problem.
46 Based on the available information on the probabilistic properties of soil [33, 51, 5, 31,
47 24, 47, 12, 40, 42, 38, 39, 14, 6, e.g.], a parametric study varying these properties is
48 presented.

49 The influence of the soil spatial variability on various geotechnical problems has al-
50 ready been investigated [19]. With respect specifically to shallow foundations, servicea-
51 bility limit states have been considered for different cases: plane strain single footing
52 [37, 19, 1], plane strain double footings [17, 2] and 3D single and double footings [18, 19];
53 these contributions used vertical loading, but inclined loads were also considered [3].
54 Moreover, the ultimate limit state problem has been deeply studied in the last years.
55 The ultimate limit state of shallow foundations resting on soils responding in undrained

56 conditions have already been greatly investigated [22, 23, 41, 13, 28, 9, 27] consider-
57 ing different probabilistic distributions for the undrained shear strength, adopting both
58 isotropic and anisotropic structures for the spatial correlations and using different meth-
59 ods to generate the random fields. Most of the works investigated only the case of a
60 vertical centered load [22, 23, 41, 13, 28, 27] and only a recent work [9] considered the
61 effect of combination of horizontal and vertical loads, together with moments. In gen-
62 eral, these works combined the use of conventional non-linear finite elements analyses or
63 numerical limit analyses with random field theory and Monte Carlo simulations.

64 The previously mentioned works have clearly shown that average bearing capacity
65 considering the soil spatial variability is smaller than the one calculating admitting an
66 homogeneous soil. However, the impact of spatial variability of soil on the safety of foun-
67 dations considering the different Design Approaches proposed in Eurocode 7 is unknown.
68 Do the Design Approaches of Eurocode 7 meet the desired level of safety for a wide range
69 of foundations when the spatial variability is considered?

70 In the present paper, reliability analysis is used to assess the level of safety of shal-
71 low foundations under undrained conditions of the Design Approaches of Eurocode 7
72 considering soil heterogeneity and the uncertainty of the eccentricity of the load. The
73 soil heterogeneity is defined by the statistical properties of the undrained shear strength,
74 c_u : mean, coefficient of variation and anisotropic correlation length. The uncertainty of
75 the load is considered through a statistical distribution of its eccentricity. The obtained
76 results are fitted to a range of probabilistic distributions for each set of parameters char-
77 acterizing the soil. These are then used to compute the reliability index using the First
78 Order Reliability Method (FORM) [48, 29] for foundations designed following Eurocode
79 7 [11].

80 2. Problem definition

81 The problem studied is a strip shallow foundation with width B on the surface of
82 undrained soil, submitted to two load cases (centered and eccentric load), as presented
83 in Figure 1. The eccentricity, e_B , of the vertical load is assumed to be described by a
84 normal distribution, being for each load case defined as:

85 Load case 1: $e_B \sim N(0; 3B/100)$

86 Load case 2: $e_B \sim N(B/6; 3B/100)$

87 The mean eccentricity considered in Load case 2 corresponds to the maximum value
88 for which, in the homogeneous case, the base of the footing remains under compression.
89 Therefore, the conclusions of the study are limited to these cases.

The bearing capacity of the foundation considering a two-dimensional plane strain
problem and a homogeneous soil can be determined by:

$$R = N_c \cdot c_u \cdot B' \quad (1)$$

where N_c is a bearing capacity factor, equal to $2 + \pi$, c_u is the undrained shear strength
and B' is the effective width, defined as:

$$B' = B - 2 \cdot e_B \quad (2)$$

90 For heterogeneous soils, no closed form expression for the bearing capacity can be defined,
91 and numerical methods must be used. As shown in Equation 1, the undrained shear

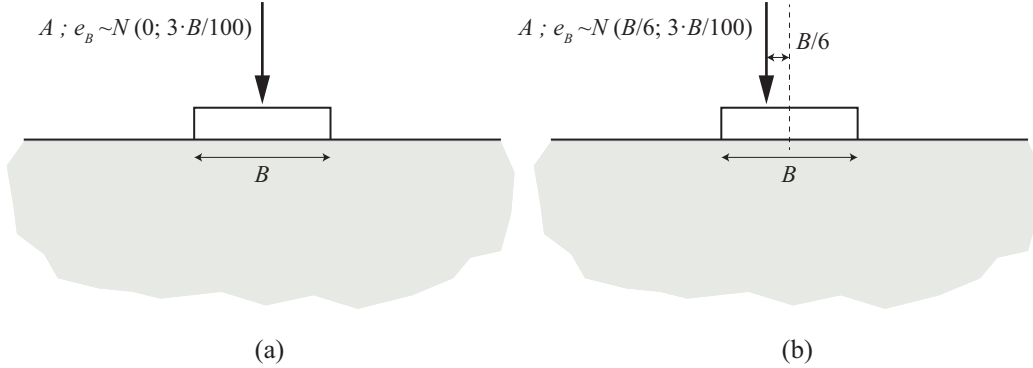


Figure 1: Scheme of the problem under study for centered (a) and eccentric load (b).

92 strength is the key parameter in the investigated problem. This is therefore the property
 93 of the soil assumed to be varying along space, representing its variability. The spatial
 94 correlation structure is characterized using both a traditional isotropic model and an
 95 anisotropic correlation structure [19].

96 3. Eurocode design

The methodology proposed in Eurocode 7 [11] is based on the application of partial safety factors increasing the effects of actions and decreasing the material strengths or the resistances. The structural safety for a given limit state is satisfied when the design value of the resistance is higher than the corresponding effect of the design actions, $R_d \geq A_d$. For the present case, considering a homogeneous soil, the design value of resistance is given by:

$$R_d = (2 + \pi) \cdot \frac{c_{u,k}}{\gamma_{c_u}} \cdot B' \cdot \frac{1}{\gamma_{R,v}} \quad (3)$$

and the design value of the actions is defined as follows:

$$A_d = \gamma_G \cdot G_k + \gamma_Q \cdot Q_k \quad (4)$$

97 where $\gamma_{R,v}$ and γ_{c_u} are the partial safety factors associated with the resistance and the
 98 undrained shear strength, respectively; $c_{u,k}$ is the characteristic value of the undrained
 99 shear strength; G_k and Q_k are the nominal values of permanent and live load, respectively,
 100 and γ_G and γ_Q are the partial safety factors associated with the permanent and live load,
 101 respectively.

102 Following Eurocode 7 [11], a set of limit states must be checked for shallow founda-
 103 tions. For the limit state GEO (failure or excessive deformation of the ground), under
 104 analysis in this work, Eurocode 7 [11] provides three alternative Design Approaches.
 105 These approaches combine different values for the partial safety factors aiming at a
 106 consistent safety level. For the structure under analysis, continuous footing on soil re-
 107 sponding in undrained conditions, the Design Approaches are:

108 **Design Approach 1 (DA1):**

- 109 • Combination 1 (*DA1.1*): $A1+M1+R1$
110 • Combination 2 (*DA1.2*): $A2+M2+R1$
111 **Design Approach 2** (*DA2*): $A1+M1+R2$
112 **Design Approach 3** (*DA3*): $(A1 \text{ or } A2)+M2+R3$

113 where “+” means “combined with” and $A1$, $A2$, $M1$, $M2$, $R1$, $R2$ and $R3$ are different
114 sets of partial factors for actions (A), material properties (M) and resistance (R). The
115 values corresponding to these sets of partial factors are presented in Tables 1 to 3.

Table 1: Partial factors for actions defined in Eurocode 7 [11] considering the GEO and STR ultimate states.

Coefficient	Type	$A1$	$A2$
γ_G	Unfavorable	1.35	1.00
	Favorable	1.00	1.00
γ_Q	Unfavorable	1.50	1.30
	Favorable	0.00	0.00

Table 2: Partial factors for vertical resistance of shallow foundations defined in Eurocode 7 [11] considering the GEO and STR ultimate states.

Structure	Resistance	Coefficient	$R1$	$R2$	$R3$
Shallow Foundation	Bearing capacity	$\gamma_{R,v}$	1.00	1.40	1.00

Table 3: Partial factors for undrained shear strength defined in Eurocode 7 [11] considering the GEO and STR ultimate states.

Coefficient	$M1$	$M2$
γ_{c_u}	1.00	1.40

116 The equations and partial factors presented show that *DA3*, considering action $A2$, is
117 equivalent to *DA1.2*, as for $R1$ and $R3$ the coefficients are both equal to 1.00. Moreover,
118 as the foundation in the problem investigated is assumed to be subjected to vertical
119 loads and to be located on the surface of a soil responding in undrained conditions,
120 *DA3*, considering action $A1$, is equivalent to *DA2*, since resistance is proportional to the
121 undrained shear strength and, applying the safety factor with the same value (1.40) to
122 the material properties or to the resistance is equivalent.

123 It should still be noted that in the case of the first Design Approach *DA1*, the second
124 combination is usually critical for limit states associated with soil failure, while the first
125 is important in the structural design of the foundations.

126 Consequently, in the following text, only *DA1.2* and *DA2* will be analyzed, and, for
 127 the present case, the only difference between *DA1.2* and *DA2* is the partial safety factor
 128 applied to actions (*A1* vs. *A2*).

129 It is common practice in some countries to consider a Design Approach *DA2** instead
 130 of *DA2*, where the effects of actions are factored instead of the actions themselves. This
 131 *DA2** was, however, not considered in the present paper.

132 4. Finite element modeling

133 The foundation analyzed in the present work represents a continuous footing with
 134 width B , equal to 1 m, and subjected to a vertical load F . The footing was considered
 135 rigid and rough. The foundation soil was modeled with dimensions equal to $5B \times 2B$,
 136 in accordance with the dimensions of soil modeled in [22, 23]. Vertical and horizontal
 137 displacements on the base of the mesh and on its left and right sides were restrained.
 138 In Figure 2, the finite element mesh used is presented. This mesh consists of 16400
 139 three node triangular elements with an element size equal to $B/20$. The elements that
 140 represent the footing are treated as a single weightless rigid body.

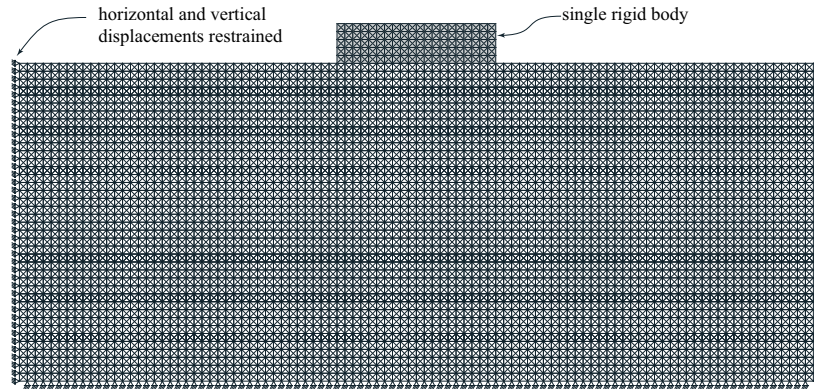


Figure 2: Mesh with a total of 16400 three node triangular elements.

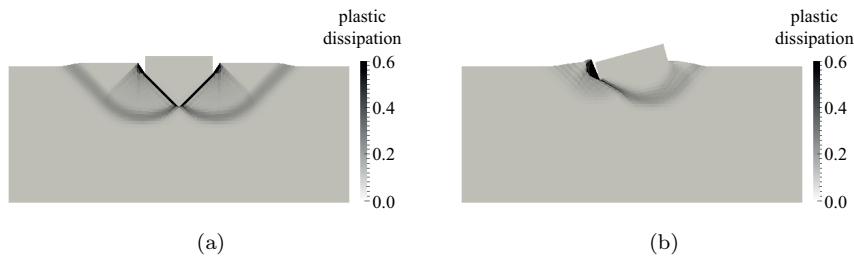


Figure 3: Collapse mechanisms using a mesh with a total of 16400 three node triangular elements for:
 (a) vertical centered load; (b) vertical load with an eccentricity equal to $B/6$.

141 In Figure 3 (a) the pattern of plastic dissipation considering a homogeneous soil and
 142 a centered load is presented, showing clearly the Prandtl mechanism for a foundation
 143 on homogeneous and isotropic ground. The collapse load obtained is $R_{Homogeneous}^{centered} =$
 144 536.1 kN/m. This corresponds to a bearing capacity factor, N_c , of 5.361, while the exact
 145 value under the conditions described is $2 + \pi$, leading to the conclusion that the finite
 146 element mesh used produces an error of 4.3% compared to the exact value. For the ec-
 147 centric load case (Figure 3 (b)) the mechanism for the homogeneous and isotropic ground
 148 is asymmetric, as expected, and the collapse load is $R_{Homogeneous}^{eccentric} = 378.5$ kN/m, which
 149 corresponds to a bearing capacity factor, N_c , of 5.678. This factor is 5.9% greater than
 150 the one obtained for centered loading. This difference can be due to the concentration of
 151 the plastic dissipation on a narrow area which would need to be more refined to obtain
 152 better results. The differences between the numerical and analytical exact results were
 153 considered admissible for the purpose of the study, as an appropriate balance between
 154 accuracy and computational time.

155 5. Reliability analysis of shallow foundations

156 Due to the heterogeneity of soil properties, in the present work soil strength is mod-
 157 elled as a random field, defined in terms of a probabilistic distribution and a correlation
 158 structure [19, e.g.]. A lognormal distribution is used along with an exponential correlation
 159 structure, described in detail in Section 5.2.

Although a range of methods have been developed over the years for evaluating struc-
 tural reliability, computing the reliability of structures whose performance is evaluated
 using complex non-linear numerical models is still a challenge. In fact, the traditional
 methods for reliability analysis include simulation (*i.e.*, Monte-Carlo simulation) and
 gradient-based methods (*e.g.*, First Order Reliability Method FORM). Simulation meth-
 ods are based on the generation of a large set of deterministic samples and the evaluation
 of the performance of each sample. The probability of failure can be computed as:

$$p_f = \frac{N_F}{N} \quad (5)$$

160 where N_F is the number of samples where failure was observed and N is the total number
 161 of samples. The main disadvantage of this method is the number of samples required for
 162 obtaining reliable results and the associated computational costs. In the present work,
 163 considering the computational cost of each numerical analysis, this method was excluded.

164 Gradient-based methods like FORM estimate the probability of failure by identifying
 165 the most likely failure point in a normalized space. A detailed description of FORM
 166 and its implementation can be found in [35]. The main disadvantage of this class of
 167 methods is the need to compute the derivatives of the performance function in order to
 168 the basic random variables. In the present work, since the performance of the foundation
 169 is computed using a complex upper bound numerical method, the accurate quantification
 170 of derivatives is impossible.

171 For these reasons, an hybrid approach was used in the present work. In a first
 172 step, the probability distribution of the resistance of the foundation is characterized
 173 using simulation. To reduce the required number of samples and, consequently, the
 174 computational cost, a variance reduction technique based on Latin Hypercube sampling

175 was employed. Based on the results of the simulation process, a probability distribution
 176 was fit to the sampled foundation resistance. This allows the definition of the limit state
 177 function as the difference between the resistance and the effect of the applied loads. This
 178 is a simple analytical expression, and FORM can be used to compute the probability of
 179 failure.

180 5.1. Simulation of random fields

181 As described above, simulation can be used to generate random fields of the undrained
 182 shear strength and, finally, compute the probabilistic distribution of the collapse load.
 183 In this work, the random field was discretized using the mid-point method [30], i.e., the
 184 space was discretized in stochastic elements and a constant value of the undrained shear
 185 strength was adopted for each stochastic mesh element. This method produces a relation
 186 between the random field and a set of correlated random variables. Simulation can then
 187 be used to generate samples of the random variables and, consequently, of the associated
 188 random field.

In order to attain accurate predictions of this distribution with a minimum number
 of samples, Latin Hypercube sampling is used [34, 36]. Although more efficient than
 pure Monte-Carlo simulation, this method requires a number of samples higher than the
 number of random variables. The simulation procedure employed followed [36]. Con-
 sidering N samples of a set of K random variables, a matrix $\mathbf{P}_{N \times K}$ where each column
 corresponds to a random permutation of $1, \dots, N$ is generated. A matrix $\mathbf{R}_{N \times K}$ of in-
 dependent uniformly distributed random numbers is also generated. This method can
 introduce spurious correlation between the random variables and, consequently, errors
 in the obtained probabilistic distribution. To remove this spurious correlation and, si-
 multaneously, to introduce the correlation structure associated with the soil properties,
 matrix \mathbf{Y} with components $y_{ij} = \Phi^{-1}\left(\frac{p_{ij}}{N+1}\right)$ is defined, where p_{ij} are the components
 of matrix $\mathbf{P}_{N \times K}$ and Φ^{-1} is the inverse of the standard normal cumulative distribution
 function. The covariance matrix of $\mathbf{Y}_{N \times K}$ is computed and Cholesky decomposed as:

$$\bar{\mathbf{L}}\bar{\mathbf{L}}^T = \text{Cov}(\mathbf{Y}) \quad (6)$$

where $\bar{\mathbf{L}}$ is lower triangular. A new matrix $\mathbf{Y}_{N \times K}^*$ is defined as follows:

$$\mathbf{Y}^* = \mathbf{Y}(\bar{\mathbf{L}}^{-1})\mathbf{L}^T \quad (7)$$

where \mathbf{L} corresponds to the Cholesky decomposition of the objective covariance matrix.
 The columns of matrix $\mathbf{P}_{N \times K}^*$ are formed by ranking the elements of each column of
 matrix $\mathbf{Y}_{N \times K}^*$. Finally, a sampling matrix $\mathbf{S}_{N \times K}$ can be computed as follows:

$$\mathbf{S} = \frac{1}{N}(\mathbf{P}^* - \mathbf{R}) \quad (8)$$

where samples are given by:

$$x_{ij} = F_{x_j}^{-1}(s_{ij}) \quad (9)$$

189 where $F_{x_j}^{-1}$ represent the inverse cumulative distribution associated with random variable
 190 j .

191 *5.2. Probabilistic characterization of soil*

192 In general, the lognormal distribution is adequate to model material strengths [26].
 193 In the case of soil properties, it is particularly useful, since variability can be very large
 194 [38], but only positive values have physical meaning [22, 6]. For these reasons, and in
 195 accordance with previous works [22, 23, 28], the undrained shear strength was defined as
 196 a lognormal distribution.

The correlation between the soil properties in two points can be modelled considering an autocorrelation function, in terms of the vertical and horizontal distance between the two points [52, 19]. In the present work, an ellipsoidal exponential autocorrelation function [52, 19] was used for the logarithm of the undrained shear strength:

$$\rho_{\ln c_u}(\Delta_V, \Delta_H) = \exp \left\{ -\sqrt{\left(\frac{2|\Delta_V|}{\theta_{\ln c_u}^V}\right)^2 + \left(\frac{2|\Delta_H|}{\theta_{\ln c_u}^H}\right)^2} \right\} \quad (10)$$

197 where $\theta_{\ln c_u}^V$ and $\theta_{\ln c_u}^H$ are the vertical and horizontal spatial correlation lengths, respec-
 198 tively, and Δ_V and Δ_H are the vertical and horizontal distances between the two points.
 199 If both spatial correlation lengths are equal, the spatial correlation structure is isotropic
 200 and, otherwise, anisotropic.

201 The spatial correlation length, or fluctuation scale, describes the homogeneity of soil,
 202 defining a distance above which the correlation is lower than a given value [50, 52].
 203 A high value of the correlation length implies a more homogeneous soil, with softer
 204 variations of the undrained shear strength. The correlation lengths can be replaced
 205 by a dimensionless parameter, denoted spatial correlation, defined as $\Theta_{\ln c_u} = \theta_{\ln c_u}/B$
 206 [22, 19], where B is the foundation width. Then, the vertical and horizontal correlation
 207 lengths can be defined in terms of the dimensionless spatial correlations, $\Theta_{\ln c_u}^V = \theta_{\ln c_u}^V/B$
 208 and $\Theta_{\ln c_u}^H = \theta_{\ln c_u}^H/B$.

209 In this work, the mean undrained shear strength will be assumed constant and equal
 210 to 100 kPa. Considering the values proposed in literature [33, 51, 5, 31, 24, 47, 12, 40,
 211 42, 38, 39, 14, 6, e.g.] for the mean value of the coefficient of variation and horizontal and
 212 vertical spatial correlation length of the undrained shear strength, the following values
 213 are assumed in the present work for these parameters:

214 $CV_{c_u} = \{0.125; 0.25; 0.5; 1\}$

215 $\Theta_{\ln c_u}^V = \{0.5; 1; 2; 4; 8\}$

216 $\Theta_{\ln c_u}^H = \{1.0\Theta_{\ln c_u}^V; 10\Theta_{\ln c_u}^V\}$

217 The heterogeneity of the soil is modelled considering the domain divided in a quadran-
 218 gular stochastic element mesh. In the generation of the samples for soil properties, four
 219 stochastic element meshes with different levels of refinement were studied as described
 220 in Table 4, with the objective of defining the minimum refinement, and, consequently,
 221 the minimum number of samples, required to ensure the correct soil spatial variabil-
 222 ity modelling. For this study, an isotropic spatial correlation structure was considered
 223 ($\Theta_{\ln c_u}^H = \Theta_{\ln c_u}^V$), as well as a vertical centered load. In Figure 4, an example for each
 224 stochastic element mesh is presented, considering $CV_{c_u} = 0.25$ and $\Theta_{\ln c_u}^V = \Theta_{\ln c_u}^H = 0.5$.

225 Figure 5 shows the mean and the standard deviation of the collapse load computed
 226 for different values of the coefficient of variation, CV_{c_u} , and of the spatial correlation,
 227 $\Theta_{\ln c_u}^V$ for the four different stochastic element meshes. Results show that a stochastic

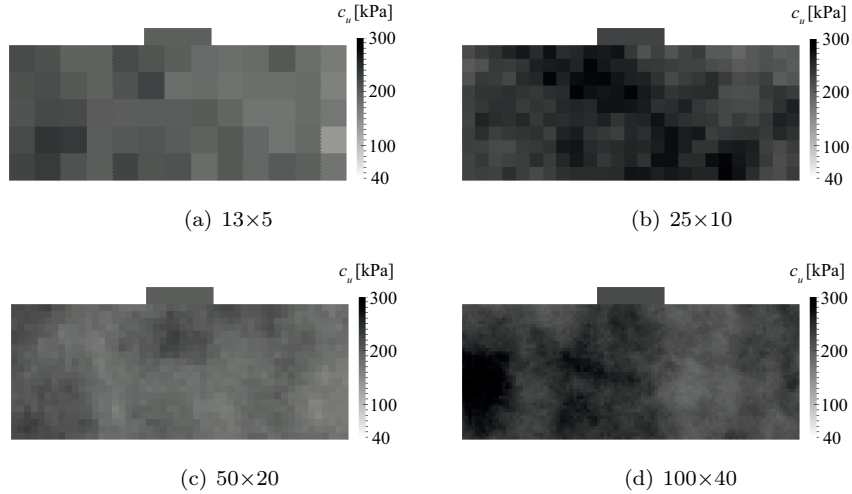


Figure 4: An example of undrained shear strength distribution for each case of stochastic element mesh studied for $CV_{c_u} = 0.25$ and $\Theta_{ln c_u}^V = \Theta_{ln c_u}^H = 0.5$.

Table 4: Stochastic element meshes studied.

Number of stochastic elements	Stochastic element width d	Number of finite elements inside of a stochastic element	Number of samples
13×5	$\sim B/2.5$	~ 256	80
25×10	$B/5$	64	300
50×20	$B/10$	16	1200
100×40	$B/20$	4	4800

228 element mesh composed by elements with dimensions equal to $d = B/10$ gives results
 229 very close to those obtained with the most refined mesh, being therefore sufficient to
 230 attain acceptable results. This mesh resulted in a minimum number of samples equal to
 231 1000, having a total of 1200 samples been used.

232 5.3. Probabilistic evaluation of bearing capacity

233 Considering the simulation procedure described, the probabilistic descriptors of the
 234 collapse load for each case of soil properties were computed. In Figure 6.a and b two
 235 samples used in the simulation procedure considering a coefficient of variation $CV_{c_u} =$
 236 0.25 and a vertical spatial correlation $\Theta_{ln c_u}^V = 2$ are presented. Figure 6.a corresponds to
 237 an isotropic distribution of undrained shear strength ($\Theta_{ln c_u}^H = \Theta_{ln c_u}^V$) and Figure 6.b to
 238 an anisotropic distribution ($\Theta_{ln c_u}^H = 10 \Theta_{ln c_u}^V$). In this case, the effect of the anisotropic
 239 correlation structure is shown by the layered distribution of properties presented. Figures

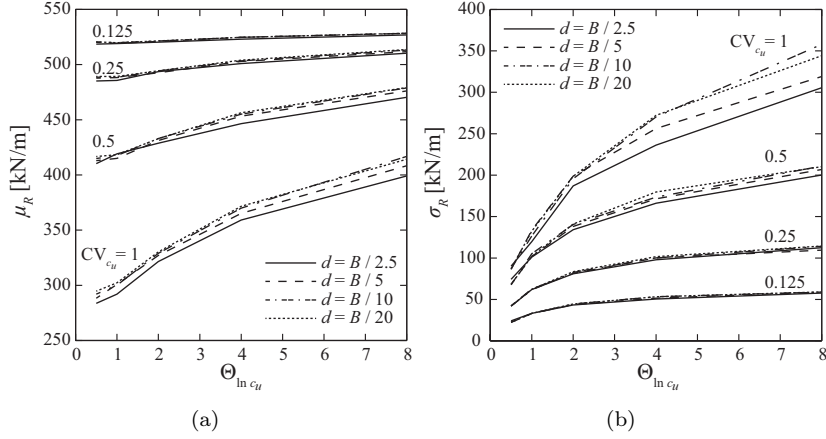


Figure 5: Evolution of mean (a) and standard deviation (b) of the bearing capacity against the value of spatial correlation for four values of the coefficient of variation and for four different stochastic element meshes, considering an isotropic spatial correlation structure.

240 6.c and d show the failure mechanisms for these two samples, when a centered vertical load
 241 is applied. The results obtained indicate that, even under a centered load, a significant
 242 asymmetry of the collapse mechanism can be observed, as a result of the heterogeneity
 243 of soil properties. However, probably due to the low coefficient of variation and spatial
 244 correlation considered, the differences in properties over the entire domain are relatively
 245 small and, as a result, the rotation of the foundation for the eccentric loading (see Figures
 246 6.e and f) is compatible with that obtained considering homogeneous soil (see Figure 3).

247 In Figure 7, two samples with a coefficient of variation $CV_{c_u} = 1$ and a vertical
 248 spatial correlation $\Theta_{ln c_u}^V = 8$ are presented considering isotropic (left) and anisotropic
 249 (right) correlation structures. This figure, when compared to Figure 6, shows the effect
 250 of increasing the correlation length on the distribution of the undrained shear strength,
 251 denoting larger areas of higher or lower strength. In the isotropic case, an area of higher
 252 strength is clearly observable on the right side of the domain, as the left side presents low
 253 strength. As a result, the failure mode is strongly asymmetric, with energy dissipation
 254 concentrated on the left side. In all cases, mechanisms show much greater complexity, as
 255 the failure surface crosses areas of lower undrained shear strength.

256 The mean normalized collapse load and the standard deviation of the collapse load
 257 computed for different values of the coefficient of variation, CV_{c_u} , and the vertical spatial
 258 correlation, $\Theta_{ln c_u}^V$, are presented in Figures 8 and 9, for isotropic and anisotropic corre-
 259 lation structures, respectively. The normalized collapse load is determined by dividing
 260 the obtained load by that determined in Section 4 associated with a homogeneous soil
 261 characterized by the mean undrained strength subjected to the same loading.

262 As previously mentioned, the bearing capacity of shallow foundations subjected to a
 263 centered vertical load and on soils responding in undrained conditions was studied in [22,
 264 23, 41, 13, 28, 9, 27]. These works showed that the soil spatial variability can significantly
 265 change the collapse mechanism and the bearing capacity. They also concluded that
 266 the normalized collapse load is lower than 1. Consistent observations are presented in

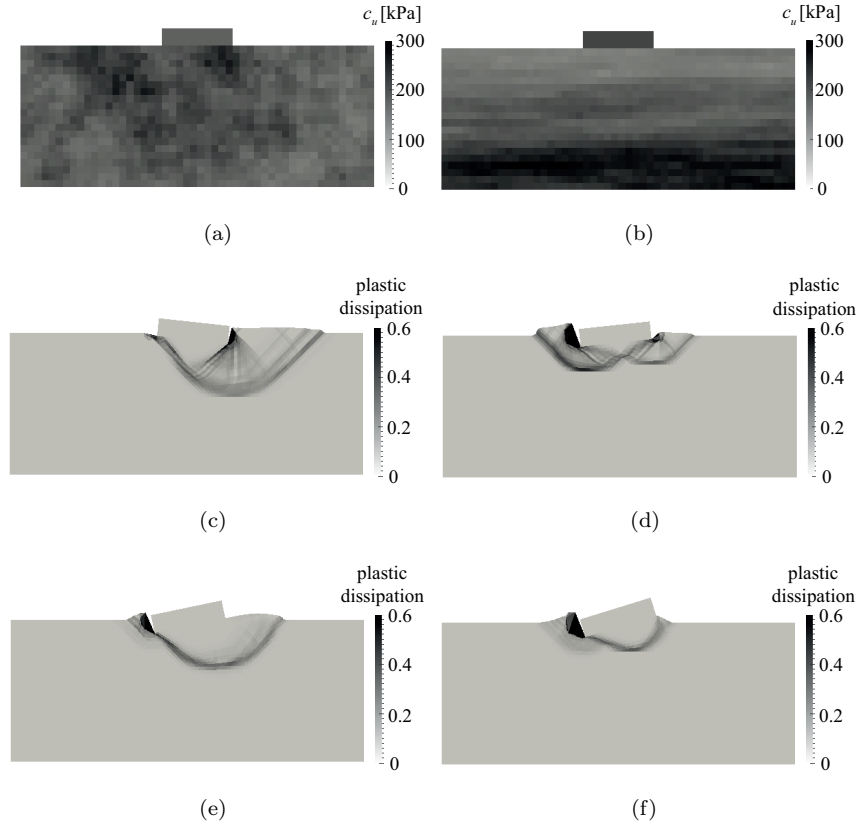


Figure 6: Examples of collapse mechanisms for both centered (c and d) and eccentric load (e and f) corresponding to an example of an undrained shear strength distribution (a and b) considering an isotropic (left) and an anisotropic spatial correlation structure (right) and for $CV_{c_u} = 0.25$ and $\Theta_{ln c_u}^V = 2$.

267 this work for centered and eccentric loads, as well as isotropic and anisotropic spatial
 268 correlation structures.

269 In fact, the results obtained in this section are justified by the observation of [22, 23]
 270 stating that the presence of weak zones in the region of interest governs the failure
 271 mechanism and, therefore, the bearing capacity of shallow foundations. The results
 272 presented show that increased uncertainty (higher CV_{c_u}) significantly reduces the mean
 273 resistance, while increasing the collapse load standard deviation. Moreover, heterogeneity
 274 (associated with low correlation lengths) leads to a reduction of the mean resistance. In
 275 fact, more heterogeneous soils are more likely to present areas of lower strength in the
 276 region of interest, and will be associated with failure mechanisms through these elements.
 277 The standard deviation of the bearing capacity increases with the correlation length. For
 278 highly correlated soil properties, large areas of lower strength exist. If, on one hand, these
 279 are located in the region of interest, a very low bearing capacity is obtained. On the
 280 other hand, if an area of higher strength is located in the region of interest, a much

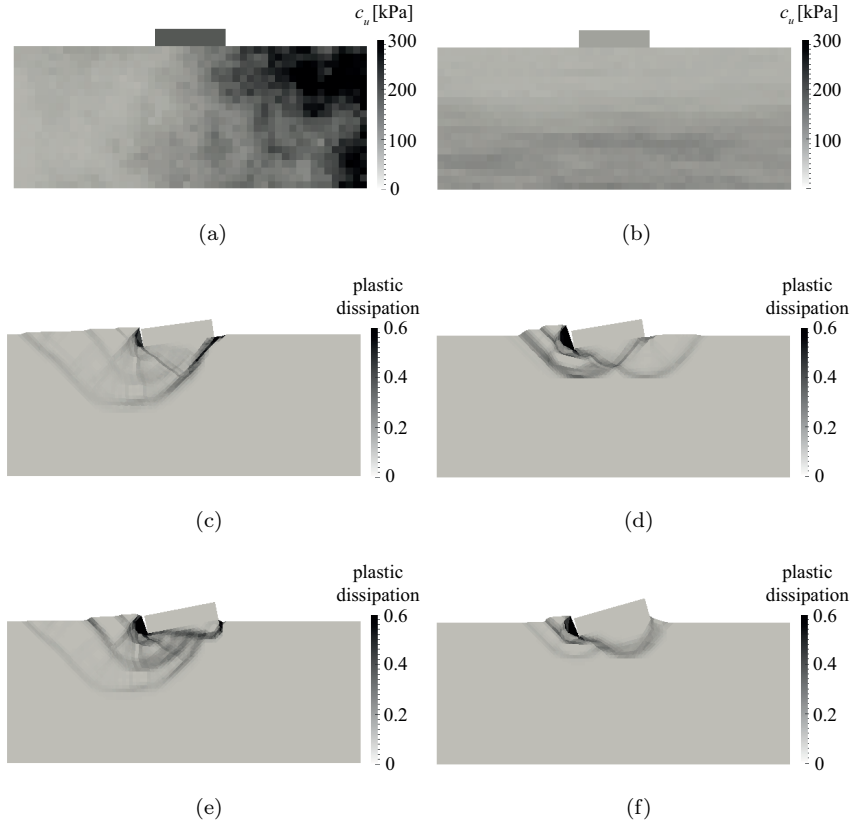


Figure 7: Collapse mechanisms for both centered (c and d) and eccentric load (e and f) corresponding to an example of an undrained shear strength distribution (a and b) considering an isotropic (left) and an anisotropic spatial correlation structure (right) and for $CV_{c_u} = 1$ and $\Theta_{ln c_u}^V = 8$.

281 higher bearing capacity results. Consequently, a larger dispersion in the distribution
 282 of the bearing capacity is obtained in this case. The difference is larger for higher
 283 coefficients of variation, as these result in greater differences between areas of lower and
 284 higher strength. The results for the anisotropic cases (Figure 9) show that an increase
 285 in the horizontal spatial correlation leads to an increase of both mean and standard
 286 deviation of the bearing capacity, which is consistent with results presented in Figure 8.

287 Although the bearing capacity under eccentric loads is lower than that obtained
 288 for centered loads, the results in Figures 8 and 9 show that the consideration of soil
 289 uncertainty has a lower impact for eccentric load scenarios, proved by the higher mean
 290 normalized bearing capacity obtained for eccentric loads. This is particularly relevant
 291 for lower coefficients of variation, for which a mean normalized capacity very close to
 292 1.00 is obtained. In terms of standard deviation, the results presented show little impact
 293 of the eccentricity of loads for lower values of CV_{c_u} ; it increases for higher coefficients of
 294 variation and higher spatial correlation.

295 The results presented show that within the range of values analyzed: (i) increasing

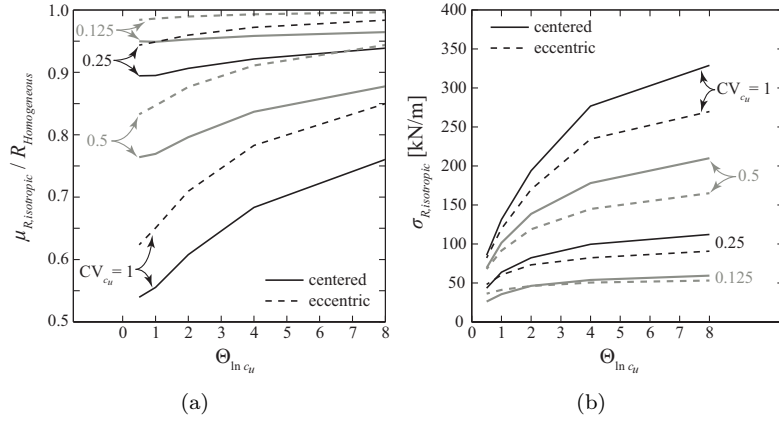


Figure 8: Evolution of normalized mean (a) and standard deviation (b) of bearing capacity against the value of spatial correlation for four coefficient of variation values and for both centered and eccentric load (as defined in Figure 1), considering an isotropic spatial correlation structure.

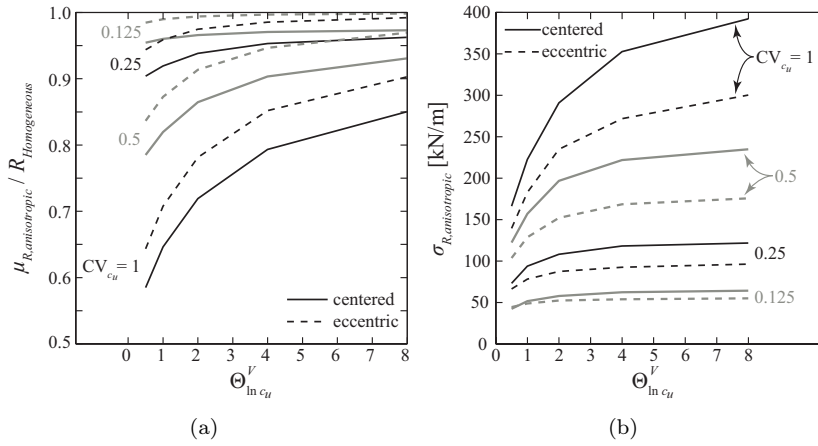


Figure 9: Evolution of normalized mean (a) and standard deviation (b) of bearing capacity against the value of spatial correlation for four coefficient of variation values and for both centered and eccentric load, considering an anisotropic spatial correlation structure with $\Theta_{ln c_u}^H = 10\Theta_{ln c_u}^V$.

296 the coefficient of variation results in lower mean values of bearing capacity; (ii) increasing
 297 spatial correlation leads to an increase of mean values of bearing capacity; (iii) higher
 298 values of the coefficient of variation and spatial correlation result in higher standard
 299 deviation of the bearing capacity. The results also show that these conclusions are valid
 300 for both centered and eccentric loads. The results obtained for the case of centered
 301 loading and isotropic spatial correlation structure are coherent with previous works on
 302 the topic [22, 23, 28], showing the consistency of the methodology applied in this work
 303 (combination of Sublim3d with Latin Hypercube sampling) to calculate the response of

304 shallow foundations.

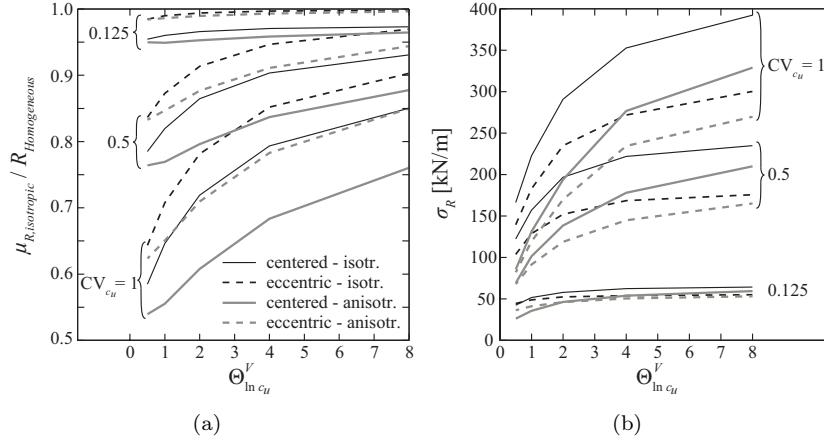


Figure 10: Comparison between the normalized mean (a) and the standard deviation (b) of bearing capacity against the value of spatial correlation for four coefficient of variation values and for both centered and eccentric load, considering an isotropic and anisotropic spatial correlation structure.

305 The comparison of results obtained for both correlation structures shows that the
 306 anisotropic spatial correlation structure results in higher values of both mean and stan-
 307 dard deviation of the bearing capacity (see Figure 10). In fact, the anisotropic structure
 308 is associated with a higher horizontal spatial correlation and, as previously observed,
 309 higher spatial correlation result in an increase of bearing capacity mean value and stan-
 310 dard deviation.

311 6. Reliability assessment of shallow foundations

312 The probabilistic analysis presented showed that the load eccentricity and coefficient
 313 of variation, correlation length and spatial correlation structure of the undrained shear
 314 strength have different, and in some cases conflicting effects, on the mean and standard
 315 deviation of the bearing capacity. A simple relation between the safety of foundations and
 316 these probabilistic descriptors is not possible. Therefore, a parametric reliability analysis
 317 was performed to analyse the dependence of the reliability index on the probabilistic
 318 descriptors of soils.

In this section, the structural safety of shallow foundations is analyzed with a reliability framework for foundations designed following Eurocode 7 [11]. The limit state function, Z , was defined as:

$$Z(R, G, Q) = R - G - Q \quad (11)$$

319 where R is the bearing capacity, G is the permanent load and Q is the live load. The
 320 bearing capacity was modelled by fitting an appropriate probability distribution for each
 321 set of results obtained in the previous section. The permanent and live load were modeled
 322 using a normal and a Gumbel distribution, respectively [7, 26, 49, 25, e.g.]. This analysis

323 presents a practical interest as it evaluates the consistency of the partial safety factors
 324 method, currently prescribed in Eurocode 7[11].

325 To model the bearing capacity, normal, lognormal, exponential, Gamma and Weibull
 326 distributions were fitted to the results described above. The probabilistic models were
 327 compared using the maximum log-likelihood function. An example of the results obtained
 328 is presented in Figure 11, where the different distribution models are fitted to the bearing
 329 capacity computed considering an isotropic spatial correlation structure with $CV_{c_u} = 0.5$
 330 and $\Theta_{ln c_u} = 4$ and a centered load. The results obtained for all the scenarios analyzed
 331 showed that the lognormal distribution resulted in adequate fit in all cases and, for this
 332 reason, was used to model the bearing capacity.

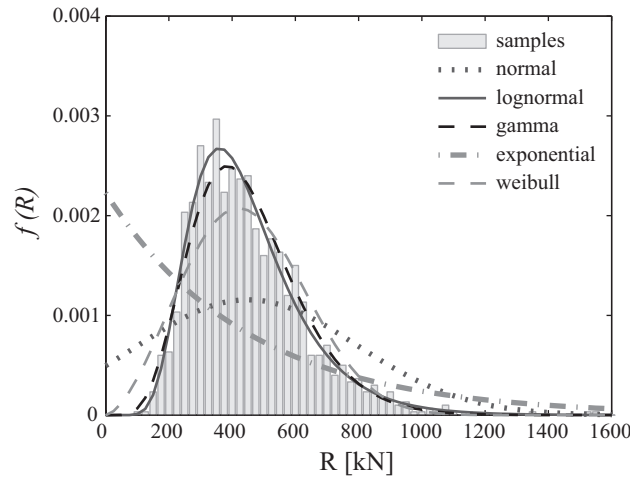


Figure 11: Foundation resistance: histogram and fitted probability distributions for the case study corresponding to an isotropic spatial correlation structure with $CV_{c_u} = 0.5$ and $\Theta_{ln c_u} = 4$ and for centered load.

333 The reliability analysis of the foundation was performed for each distribution of the
 334 undrained shear strength and each Eurocode Design Approach, considering different
 335 ratios between dead and live loads ($Q_k/(Q_k + G_k)$). Each distribution of the undrained
 336 shear strength results in a different nominal value of strength, $c_{u,k}$ computed herein as
 337 the 5% percentile of the associated distribution. Based on this and on the partial safety
 338 factors associated with each Design Approach, the design foundation resistance R_d can
 339 be computed as:

$$R_d = (2 + \pi) \cdot B' \cdot \frac{c_{u,k}}{\gamma_{c_u}} \cdot \frac{1}{\gamma_{R;v}} \quad (12)$$

340 Based on this and the the ratios between dead and live loads, the maximum nominal
 341 loads which can safely be applied, according to Eurocode 7 [11], are:

$$A_d = \gamma_G \cdot G_k + \gamma_Q \cdot Q_k \leq R_d \quad (13)$$

From these, the probability distribution of the dead load and the live load to be used in the reliability analysis can be computed assuming that the permanent load is

characterized by a normal distribution with a coefficient of variation equal to 10% while the live load can be modeled appropriately by a Gumbel distribution with a coefficient of variation equal to 35% [7, 26, 49, 25, e.g.]. If all variables were independent and normally distributed, the reliability index could be computed as:

$$\beta = \Phi^{-1}(p_f) = \frac{\mu_R - \mu_G - \mu_Q}{\sqrt{\sigma_R^2 + \sigma_G^2 + \sigma_Q^2}} \quad (14)$$

342 where μ_R , μ_G and μ_Q are the mean of the normal distribution which characterize the
 343 resistance, permanent load and live load, respectively, and σ_R , σ_G and σ_Q are the cor-
 344 respondent standard deviations. In the present case, as the variables are non-Gaussian,
 345 this expression results only in an estimate of the reliability index. Consequently, the re-
 346 liability index was computed using *iForm* [48], implemented in the open-source program
 347 *FERUM* (Finite Element Reliability Using Matlab) [8, 29].

348 Figure 12 shows the reliability index obtained considering both Design Approaches
 349 and an isotropic spatial correlation structure. The obtained reliability indices vary signif-
 350 icantly, as wide ranges of coefficients of variation (CV_{c_u}) and spatial correlation ($\Theta_{ln c_u}$)
 351 are considered.

352 The results show, as expected, that increasing the coefficient of variation (CV_{c_u}) or
 353 the spatial correlation ($\Theta_{ln c_u}$) leads to a reduction in the reliability index. In fact, as
 354 shown in Figure 10, increasing either of these parameters leads to an increase in the
 355 standard deviation of the bearing capacity, which, considering equation 14, results in a
 356 reduction of the reliability index. These results also show that the ratio between live
 357 and total load influences the reliability index. However, except for very low spatial
 358 correlation ($\Theta_{ln c_u} = 0.5$) or very low coefficients of variation of the undrained shear
 359 strength ($CV_{c_u} = 0.125$), the reliability index is relatively uniform, showing that the
 360 partial safety factors for loads defined in Eurocode 7 [11] are adequate.

361 The decrease of the reliability index with the increasing of the spatial correlation is
 362 more evident for the isotropic than for the anisotropic correlation structure, which results
 363 from the greater influence of this parameter in the standard deviation value of bearing
 364 capacity for the first type of correlation structure (see Figure 10). It can also be seen that
 365 the trend previously mentioned (i.e. higher values of reliability index for lower values of
 366 spatial correlation) is more evident for higher values of the coefficient of variation, which
 367 also has the same explanation. For both structures and both loads, the influence of the
 368 spatial correlation is higher for greater values of the coefficient of variation.

369 Comparing the two Design Approaches considered, the only difference, for the struc-
 370 ture under analysis, lies on the lower load partial safety factors used for *DA1.2*. From
 371 equation 13, this results in higher mean loads and, consequently, higher standard de-
 372 viations of loads for *DA1.2*. This increase in mean and standard deviation of design
 373 foundation resistance leads to a lower reliability index (see equation 14). Since in equa-
 374 tion 14 the square root of the sum of the squared standard deviations is considered,
 375 the effect of the increase in standard deviation of loads is reduced when the uncertainty
 376 in load bearing capacity (σ_R) increases. As a result, as shown in Figure 12, the re-
 377 liability indices obtained using *DA1.2* (left) are always lower than those resulting from
 378 *DA2* (right), but this difference is reduced for higher coefficients of variation and spatial
 379 correlations.

380 The results obtained considering an anisotropic correlation structure (Figure 13) show

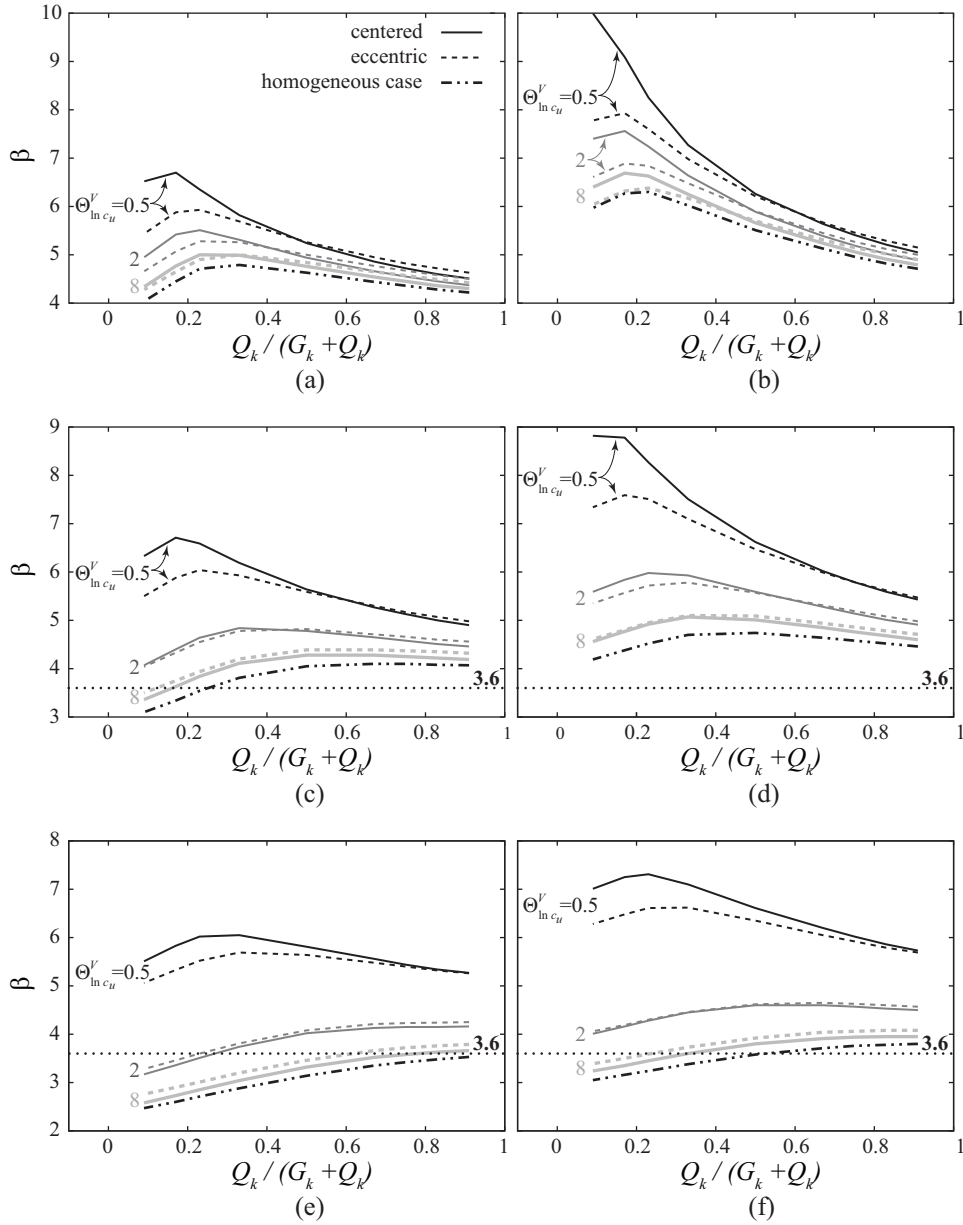


Figure 12: Evolution of reliability index against loads ratio for an isotropic spatial correlation structure with CV_{c_u} equal to 0.125 (a and b), 0.25 (c and d) and 0.5 (e and f), considering the DA1.2 (left) and the DA2 (right).

381 a lower reliability index than those obtained for the isotropic case. This is a direct
 382 consequence of the higher standard deviation of the bearing capacity resulting from

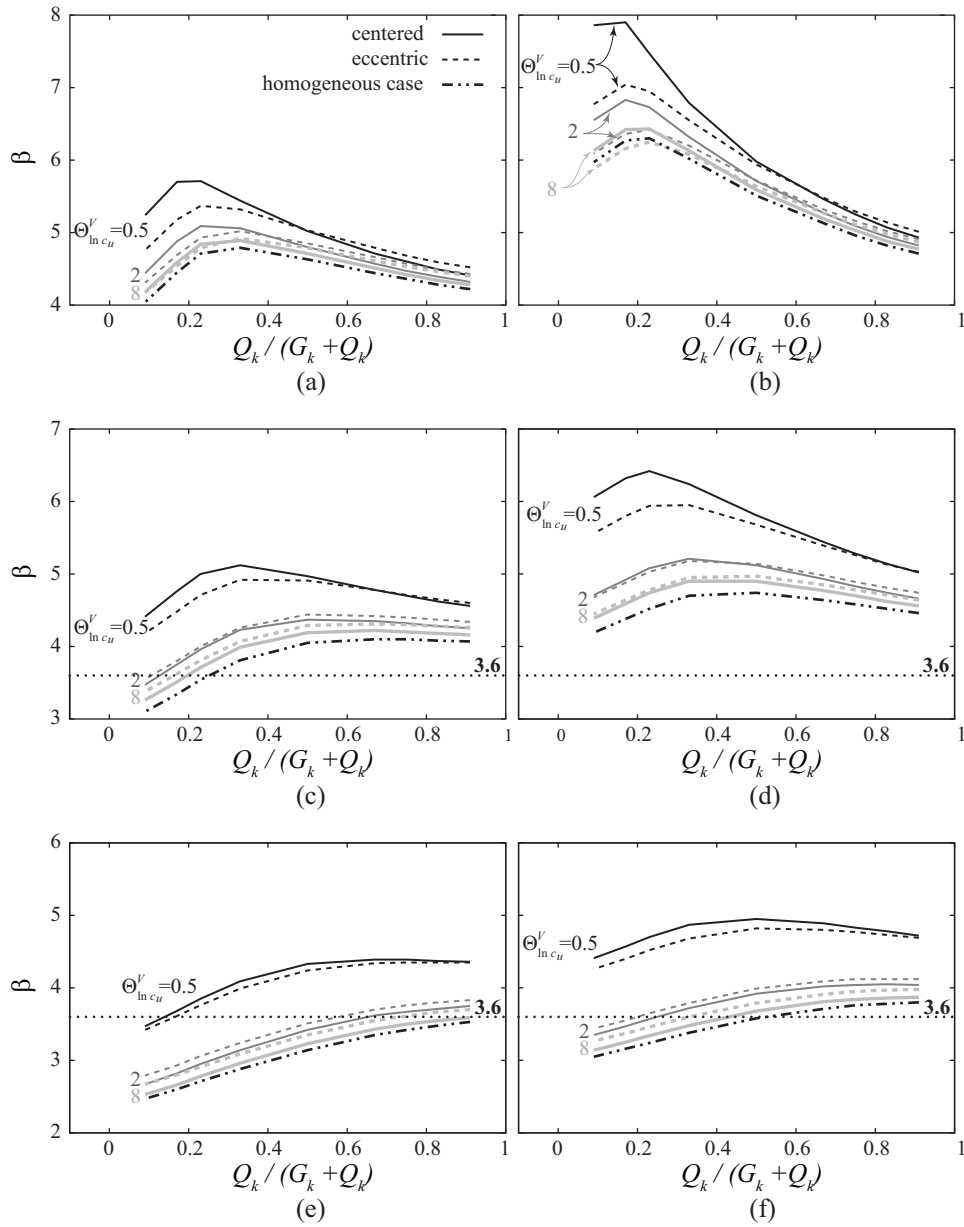


Figure 13: Evolution of reliability index against loads ratio for an anisotropic spatial correlation structure with CV_{c_u} equal to 0.125 (a and b), 0.25 (c and d) and 0.5 (e and f), considering the DA1.2 (left) and the DA2 (right).

383 anisotropy.

384 The comparison of the results obtained under a centered and an eccentric load show

385 very small differences, indicating that the approach used in Eurocode 7 [11] for assessing
386 the safety of eccentric loaded shallow foundations is consistent.

387 In Figures 12 and 13, the reliability index obtained assuming a homogeneous soil
388 ($\theta_{ln c_u} \rightarrow \infty$) and an analytical limit state function are also presented. In all examples
389 analyzed, assuming a homogeneous soil leads to lower safety levels, as a result of the
390 increase in bearing capacity standard deviation. Therefore, analytical models assuming
391 homogeneous soil can be regarded as a simple but conservative approach to the safety
392 analysis of shallow foundation.

393 Comparing the reliability indices computed with the threshold defined in Eurocode
394 0 [10] ($\beta_{target} = 3.6$), it can be seen that *DA2* leads to acceptable safety levels, except
395 if lower values of live load to total load ratios, high coefficient of variation and spatial
396 correlation are considered for the undrained shear strength. On the other hand, the
397 use of Design Approach *DA1.2* leads to undesirable safety levels for a wide range of
398 probabilistic soil properties, presenting the same trends as seen for the Design Approach
399 *DA2*.

400 7. Conclusions

401 In the present work a reliability assessment of shallow foundations subjected to ver-
402 tical loads, responding in undrained conditions, considering explicitly the soil spatial
403 variability was carried out. Firstly, random fields representing the soil, considering dif-
404 ferent coefficients of variation, both vertical and horizontal spatial correlation lengths and
405 soil spatial correlation structure were generated using Latin Hypercube sampling. Re-
406 garding to the shallow foundations bearing capacity response, it is important to highlight
407 that:

- 408 • the mean value of the bearing capacity increases with decreasing coefficients of vari-
409 ation and increasing spatial correlation lengths. The standard deviation value of
410 the bearing capacity increases with increasing coefficients of variation and spatial
411 correlation lengths. These trends were observed for both centered and eccentric
412 loadings, as well as isotropic and anisotropic distributions of the spatial variability.
413 These observations are consistent with previous works focusing on the same topic
414 [22, 23, 41, 13, 28, 9, 27], which confirms that the combination of the Latin Hyper-
415 cube sampling [34, 36] with Sublim3d [45] is suitable to investigate the influence of
416 soil heterogeneity in the bearing capacity of foundations [46];
- 417 • the ratio between the mean value of the bearing capacity and the bearing capacity
418 value determined considering a homogeneous soil is similar for centered and eccen-
419 tric loads. Regarding to the standard deviation, the values obtained tend to be
420 smaller for the eccentric load;
- 421 • the results obtained for an anisotropic spatial correlation structure are consistent
422 with those expected when there is an increase in the spatial correlation length,
423 i.e., comparing the results obtained for both spatial correlation structures, greater
424 values of mean and standard deviation values of the bearing capacity are verified
425 for the anisotropic structure (for the same vertical scale of fluctuation).

426 With the bearing capacity response reliability index following Eurocode 7 [11] ap-
427 proaches were calculated based on *iForm* [48] implemented on the open-source program
428 *FERUM* [8]. With respect to the results obtained for the reliability index, the main
429 conclusions are:

- 430 • *DA2* leads always to larger values of reliability index as consequence of its greater
431 values for partial safety factors;
- 432 • *DA1.2* leads to undesirable safety levels for a wide range of probabilistic soil prop-
433 erties, presenting, nevertheless, the same trends as seen for the Design Approach
434 *DA2*;
- 435 • the difference between the two approaches will increase if the base of the foundation
436 is below the surface, as is usually the case in practice;
- 437 • the results have shown very small differences between centered and eccentric load;
- 438 • the approach used in Eurocode 7 [11] for assessing the safety of eccentric loaded
439 shallow foundations is consistent;
- 440 • for the cases analysed in the present work, reliability analysis using analytical
441 models assuming homogeneous soil can be regarded as a simple but conservative
442 approach to the safety analysis of shallow foundations;

443 Acknowledgments

444 The authors acknowledge the support of the Geotechnical Group of the Department of
445 Civil Engineering of the Universidade Nova de Lisboa and UNIC - Centro de Investigação
446 em Estruturas e Construção. The second author acknowledges the support of Fundação
447 para a Ciência e Tecnologia through grant PTDC/ECM/115932/2009.

448 References

- 449 [1] Ahmed, A., Soubra, A.H.: Probabilistic analysis of strip footings resting on a spatially random
450 soil using subset simulation approach. *Georisk* **6**, 188–201 (2012)
- 451 [2] Ahmed, A., Soubra, A.H.: Probabilistic analysis at serviceability limit state of two neighboring strip
452 footings resting on a spatially random soil. *Structural Safety* **49**, 2–9 (2014)
- 453 [3] Al-Bittar, T., Soubra, A.H.: Probabilistic analysis of strip footings resting on spatially varying
454 soils and subjected to vertical or inclined loads. *Journal of Geotechnical and Geoenvironmental*
455 *Engineering* **140**(4) (2014)
- 456 [4] Antão, A.N., Vicente da Silva, M., Guerra, N.M.C., Delgado, R.: An upper bound-based solution
457 for the shape factors of bearing capacity of footings under drained conditions using a parallelized
458 mixed f.e. formulation with quadratic velocity fields. *Computers and Geotechnics* **41**, 23–35 (2012)
- 459 [5] Asoaka, A., Grivas, D.: Spatial variability of the undrained strength of clays. *Journal of Engineering*
460 *Mechanics* **108**(5), 743–756 (1982). ASCE
- 461 [6] Baecher, G.B., Christian, J.T.: *Reliability and Statistics in Geotechnical Engineering*. John Wiley
462 and Sons (2003)
- 463 [7] Bartlett, F.M., Hong, H.P., Zhou, W.: Load factor calibration for the proposed 2005 edition of the
464 national building code of canada: Statistics of loads and load effects. *Canadian Journal of Civil*
465 *Engineering* **30**(2), 429–439 (2003)
- 466 [8] Bourinet, J.M.: *Ferum 4.1 user's guide* (2010)
- 467 [9] Cassidy, M.J., Uzielli, M., Tian, Y.: Probabilistic combined loading failure envelopes of a strip
468 footing on spatially variable soil. *Computers and Geotechnics* **49**, 191–205 (2013)

- 469 [10] CEN: EN 1990:2009, Eurocode 0 - Basis of structural design. European Committee for Standard-
470 ization (2009)
- 471 [11] CEN: EN 1997-1:2010, Eurocode 7 - Geotechnical design. European Committee for Standardization
472 (2010)
- 473 [12] Chiasson, P., Lafleur, J., Soulié, M., Law, K.T.: Characterizing spatial variability of a clay by
474 geostatistics. *Canadian Geotechnical Journal* **32**, 1–10 (1995)
- 475 [13] Cho, S.E., Park, H.C.: Effect of spatial variability of cross-correlated soil properties on bearing
476 capacity of strip footing. *International Journal for Numerical and Analytical Methods in Geome-*
477 *chanics* **34**, 1–26 (2010)
- 478 [14] Duncan, J.M.: Factors of safety and reliability in geotechnical engineering. *Journal of Geotechnical*
479 *and Geoenvironmental Engineering* **126**, 307–316 (2000)
- 480 [15] Fenton, G.A.: Simulation and analysis of random fields. Ph.D. thesis, Department of Civil Engi-
481 neering and Operations Research, Princeton University (1990)
- 482 [16] Fenton, G.A.: Error evaluation of three random-field generators. *Journal of engineering mechanics*
483 **120**(12), 2478–2497 (1994)
- 484 [17] Fenton, G.A., Griffiths, D.V.: Probabilistic foundation settlement on a spatially random soil. *Jour-*
485 *nal of Geotechnical and Geoenvironmental Engineering* **128**(5), 381–390 (2002). ASCE
- 486 [18] Fenton, G.A., Griffiths, D.V.: Three-dimensional probabilistic foundation settlement. *Journal of*
487 *Geotechnical and Geoenvironmental Engineering* **131**(2), 232–239 (2005). ASCE
- 488 [19] Fenton, G.A., Griffiths, D.V.: *Risk Assessment in Geotechnical Engineering*. John Wiley and Sons,
489 New York (2008)
- 490 [20] Fenton, G.A., Vanmarcke, E.: Simulation of random fields via local average subdivision. *Journal of*
491 *Engineering Mechanics* **116**(8), 1733–1749 (1990). ASCE
- 492 [21] Florian, A.: An efficient sampling scheme: Updated latin hypercube sampling. *Probabilistic Engi-*
493 *neering Mechanics* **7**, 123–130 (1992)
- 494 [22] Griffiths, D.V., Fenton, G.A.: Bearing capacity of spatially random soil: the undrained clay prandtl
495 problem revisited. *Géotechnique* **51**(4), 351–359 (2001)
- 496 [23] Griffiths, D.V., Fenton, G.A., Manoharan, N.: Bearing capacity of rough rigid strip footing on
497 cohesive soil: Probabilistic study. *ASCE Journal Geotechnical and Geoenvironmental Engineering*
498 **128**(9), 743–755 (2002)
- 499 [24] Harr, M.E.: *Reliability based design in civil engineering*. McGraw Hill, London, New York (1987)
- 500 [25] Holicky, V., Markova, J., Gulvanessian, H.: Code calibration allowing for reliability differentia-
501 tion and production quality. In: *Application of Statistics and Probability in Civil Engineering:*
502 *Proceedings of the 10th International Conference*. Kanda, Takada and Furuat (2007)
- 503 [26] JCSS: JCSS Probabilistic Model Code. Part 2: Load Models. Joint Committee on Structural Safety
504 (2001)
- 505 [27] Jha, S.: Reliability-based analysis of bearing capacity of strip footings considering anisotropic
506 correlation of spatially varying undrained shear strength. *International Journal of Geomechanics*
507 (2016)
- 508 [28] Kasama, K., Whittle, A.J.: Bearing capacity of spatially random cohesive soil using numerical limit
509 analyses. *Journal of Geotechnical and Geoenvironmental Engineering* **137**(11), 989–996 (2011)
- 510 [29] Kiureghian, A.D., Haukaas, T., Fujimura, K.: Structural reliability software at the university of
511 california, berkeley. *Structural Safety* **28**(1), 44–67 (2006)
- 512 [30] Kiureghian, A.D., Ke, J.B.: The stochastic finite element method in structural reliability. *Proba-*
513 *bilistic Engineering Mechanics* **3**(2), 83–91 (1988)
- 514 [31] Lee, I., White, W., Ingles, O.: *Geotechnical Engineering*. Pitman, London (1983)
- 515 [32] Low, B.K., Phoon, K.K.: Reliability-based design and its complementary role to eurocode 7 design
516 approach. *Computers and Geotechnics* **65**, 30–44 (2015)
- 517 [33] Lumb, P.: The variability of natural soils. *Canadian Geotechnical Journal* **3**, 74–97 (1966)
- 518 [34] McKay, M.D., Beckman, R.J., Conover, W.J.: A comparison of three methods for selecting values
519 of input variables in the analysis of output from a computer code. *Technometrics* **21**(2), 239–245
520 (1979)
- 521 [35] Melchers, R.E., Beck, A.T.: *Structural reliability analysis and prediction*. John Wiley & Sons
522 (2018)
- 523 [36] Olsson, A., Sandberg, G., Dahlblom, O.: On latin hypercube sampling for structural reliability
524 analysis. *Structural Safety* **25**(1), 47–68 (2003)
- 525 [37] Paice, G.M., Griffiths, D.V., Fenton, G.A.: Finite element modeling of settlements on spatially
526 random soil. *Journal of Geotechnical Engineering* **122**(9), 777–779 (1996)
- 527 [38] Phoon, K.K., Kulhawy, F.H.: Characterization of geotechnical variability. *Canadian Geotechnical*

- Journal **36**(3), 612–624 (1999)
- 529 [39] Phoon, K.K., Kulhawy, F.H.: Evaluation of geotechnical property variability. *Canadian Geotechnical Journal* **36**(3), 625–639 (1999)
- 530 [40] Popescu, R.: Stochastic variability of soil properties: data analysis, digital simulation, effects on system behaviour. Ph.D. thesis, Princeton University, USA (1995)
- 531 [41] Popescu, R., Deodatis, G., Nobahar, A.: Effects of random heterogeneity of soil properties on bearing capacity. *Probabilistic Engineering Mechanics* **20**(4), 324–341 (2005)
- 532 [42] Popescu, R., Prevost, J.H., Deodatis, G.: Effects of spatial variability on soil liquefaction: some design recommendations. *Géotechnique* **47**, 1019–1036 (1997)
- 533 [43] Vicente da Silva, M.: Implementação numérica tridimensional do teorema cinemático da análise limite. Ph.D. thesis, Faculdade de Ciências e Tecnologia da Universidade Nova de Lisboa, Lisboa (2009). In Portuguese
- 534 [44] Vicente da Silva, M., Antão, A.N.: A non-linear programming method approach for upper bound limit analysis. *International Journal for Numerical Methods in Engineering* **72**, 1192–1218 (2007)
- 535 [45] Vicente da Silva, M., Antão, A.N.: Upper bound limit analysis with a parallel mixed finite element formulation. *International Journal of Solids and Structures* **45**, 5788–5804 (2008)
- 536 [46] Simões, J.T., Neves, L.C., Antão, A.N., Guerra, N.M.C.: Probabilistic analysis of bearing capacity of shallow foundations using three-dimensional limit analyses. *International Journal of Computational Methods* **11**(2), 1342,008–1–20 (2014)
- 537 [47] Soulié, M., Montes, M., Silvestri, V.: Modelling spatial variability of soil parameters. *Canadian Geotechnical Journal* **27**, 617–630 (1990)
- 538 [48] Sudret, B., Kiureghian, A.D.: Stochastic Finite Element Methods and Reliability, A State-of-the-Art Report. Department of Civil and Environmental Engineering, University of California, Berkeley (2000)
- 539 [49] Teixeira, A., Correia, A.G., Honjo, Y., Henriques, A.A.: Reliability analysis of a pile foundation in a residual soil: contribution of the uncertainties involved and partial factors. In: 3rd International Symposium on Geotechnical Safety and Risk (ISGSR2011). Munich, Germany: Vogt, Schuppener, Straub and Bräu (2011)
- 540 [50] Vanmarcke, E.: Probabilistic modeling of soil profiles. *Journal of the Geotechnical Engineering Division* **103**(11), 1227–1246 (1977). ASCE
- 541 [51] Vanmarcke, E.: Reliability of earth slopes. *Journal of the Geotechnical Engineering Division* **103**(11), 1247–1265 (1977). ASCE
- 542 [52] Vanmarcke, E.: *Random Fields: Analysis and Synthesis*. Princeton University, USA (2010)
- 543 [53] Whitman, R.V.: Organizing and evaluating uncertainty in geotechnical engineering. *Journal of Geotechnical and Geoenvironmental Engineering* **126**(7), 583–593 (2000)